

---

# A MODIFIED DEEP CONVOLUTIONAL NEURAL NETWORK FOR DETECTING COVID-19 AND PNEUMONIA FROM CHEST X-RAY IMAGES BASED ON THE CONCATENATION OF XCEPTION AND RESNET50V2

---

**Mohammad Rahimzadeh**

School of Computer Engineering  
Iran University of Science and Technology, Iran

[mr7495@yahoo.com](mailto:mr7495@yahoo.com)

ORCID: [0000-0002-8550-8967](https://orcid.org/0000-0002-8550-8967)

Corresponding author

**Abolfazl Attar**

Department of Electrical Engineering  
Sharif University of Technology, Iran

[attar.abolfazl@ee.sharif.edu](mailto:attar.abolfazl@ee.sharif.edu)

ORCID: [0000-0001-6727-432X](https://orcid.org/0000-0001-6727-432X)

October 29, 2021

## ABSTRACT

In this paper, we have trained several deep convolutional networks with the introduced training techniques for classifying X-ray images into three classes: normal, pneumonia, and COVID-19, based on two open-source datasets. Our data contains 180 X-ray images that belong to persons infected to COVID-19, so we tried to apply methods to achieve the best possible results. In this research, we introduce some training techniques that help the network learn better when we have an unbalanced dataset (fewer cases of COVID-19 along with more cases from other classes). We also propose a neural network that is a concatenation of Xception and ResNet50V2 networks. This network achieved the best accuracy by utilizing multiple features extracted by two robust networks. For evaluating our network, we have tested our network on 11302 images to report the actual accuracy our network can achieve in real circumstances. The average accuracy of the proposed network for detecting COVID-19 cases is 99.50%, and the overall average accuracy for all classes is 91.4%.

**Keywords** Deep learning · Convolutional Neural networks · COVID-19 · Coronavirus · Transfer Learning · deep feature extraction · chest X-ray images

## 1 Introduction

The pervasive spread of the coronavirus around the world has quarantined many people and crippled many industries, which has had a devastating effect on human life quality. So far, the coronavirus has killed at least 1.5 million patients and at least 80,000 people [19]. Due to the high transmissibility of coronavirus, the detection of this disease (COVID-19) plays an important role in controlling and planning to prevent it.

On the other hand, demographic conditions such as age and sex of individuals and many urban parameters such as temperature and humidity affect the prevalence of this disease in different parts of the world, which is more effective in spreading this disease [22, 21].

The lack of detective tools and the limitations in their production has slowed down the disease detection; as a result, it increases the number of patients and casualties. The incidence of other diseases and the prevalence and the number of casualties due to COVID-19 disease will decrease if it is detected quickly.

The first step is to get the detection, recognize the symptoms of the disease, and use distinctive signs to detect the coronavirus accurately. Depending on the type of coronavirus, symptoms can range from symptoms of the common

cold to fever, cough, shortness of breath, and acute respiratory problems. The patient may also have a few days of cough for no apparent reason[32].

Unlike SARS, coronavirus affects not only the respiratory system but also other vital organs in the body, such as the kidneys and liver [18]. Symptoms of a new coronavirus leading to COVID-19 usually begin a few days after the person becomes infected, where, in some people, the symptoms may appear a little later. According to [13, 36], Respiratory problems are one of the main symptoms of COVID-19, which can be detected by the X-ray imaging of the chest. CT scans of the chest can also show a disease that has mild symptoms, so analyzing these images can well detect the presence of the disease in suspicious people and even without symptoms at first [29]. Using these data can also cover the limitations of other tools, such as the lack of diagnostic kits and the limitations of their production. The advantage of using CT scans and X-ray images is the availability of CT scan devices and x-ray imaging systems in most hospitals and laboratories, and the ease of access to the data needed to train the network and thus detect the disease. In the absence of common symptoms such as fever, the use of CT scans and X-ray images of the chest has a relatively good ability to detect the disease [1].

The use of specialized human beings to diagnose the disease is a common method of detecting COVID-19 in laboratories. In this method, the specialist uses the symptoms and injuries in the chest radiology image to detect COVID-19 disease from a healthy person or person that suffering from other diseases. This procedure has costs and, most importantly, long-term detection [13, 28].

In recent years, computer vision and Deep Learning have been used to detect many different diseases and lesions in the body automatically [17].

Some examples are: Detection of tumor types and volume in lungs, breast, head and brain [3, 14], state-of-the-art bone suppression in x-rays, diabetic retinopathy classification, prostate segmentation, nodule classification [17], skin lesion classification, analysis of the myocardium in coronary CT angiography [40], sperm detection and tracking [24], etc.

Given that chest CT scan or X-ray images analysis is one of the methods of diagnosing COVID-19, the use of computer vision and Deep Learning can play a beneficial role in diagnosing this disease. Since the disease became widespread, many researchers have used machine vision and Deep Learning methods and obtained good results.

Due to the sensitivity of the Covid-19 diagnosis, the diagnosis's accuracy is one of the main challenges we face in our research. On the other hand, our focus is on increasing the detection efficiency due to the limited open-source data available.

In this article, we try to improve COVID-19 detection and decreasing wrong COVID-19 detections. This is done by combining two robust deep convolutional neural networks and optimizing the training parameters. Besides, we also propose a method for training the network when the dataset is imbalanced.

In [1, 38], statistical analysis of CT scans was performed by several specialists and diagnosticians, who classified the suspects into several classes for diagnosis and treatment.

Because of the superiority of computer vision and Deep Learning in the analysis of medical images, after the reliability of CT scans of the chest for COVID-19 detection, the researchers used these tools to diagnose COVID-19. Immediately, artificial intelligence began to detect the disease and measure the rate of infection and damage to the lungs using CT scans and the course of the disease, with promising results [9].

IN [34], they have used an innovative CNN to classify and predict COVID-19 using lung CT scans. [9] has used Deep Learning to detect COVID-19 and segment the lung masses caused by the coronavirus using 2D and 3D images. COVID-Net uses a lightweight residual projection-expansion- projection-extension (PEPX) design pattern to investigate quantitative analysis and qualitative analysis [33]. In another research, pre-trained ResNet50, InceptionV3, and Inception ResNetV2 models have used with transfer learning techniques to classify Chest X-ray images normal and COVID-19 classes [20]. In [15], they present COVNet for predict COVID-19 from CT scans that have segmented using U-net [25].

Another research has combined the Human-In-The-Loop(HITL) strategy that involved a group of chest radiologists with deep learning-based methods to segment and measure infection in CT scans [26]. In [37], they have tried to detect COVID-19 and Influenza-A-viral-pneumonia from their data; They have used classical ResNet-18 network structure to extract the features, and another Innovative CNN network uses these features by creating the location-attention oriented model to classify the data.

The paper is organized as follows: In Section 2, we describe the proposed neural network, the dataset, and training techniques. In Section 3, we have presented the experimental results, and then the paper is discussed in Section 4. In Section 5, we concluded our paper, and in 6, we presented the trained networks and the codes used in this research.

## 2 Methodology

### 2.1 Neural Networks

Deep convolutional neural networks have made a mutation in machine vision tasks. These layers have created advances in many field like Agriculture [23], medical disease diagnosis [16, 35], industry [7]. The superiority of these networks comes from the robust and valuable semantic features they generate from the input data. Here the main job of the deep networks is detecting the infections and the kind of those in the X-ray images, so classifying the X-ray images into normal, pneumonia or COVID-19. Some of the powerful and mostly used deep convolutional networks are VGG [27], ResNet [10], DenseNet [12], Inception [31], Xception [4].

Xception is a deep convolutional neural network that introduced new inception layers. These inception layers are constructed from depthwise separable convolution layers, followed by a point-wise convolution layer. Xception achieved the third-best results on the ImageNet dataset [8] after InceptionresnetV2 [30] and NasNet Large [39]. ResNet50V2 [11] is a modified version of ResNet50 that performs better than ResNet50 and ResNet101 on the Imagenet dataset. In ResNet50V2, a modification was made in the propagation formulation of the connections between the blocks. ResNet50V2 also achieves a good result on the ImageNet dataset.

The pre-processed input images of our dataset are 300\*300 pixels. Xception generates a 10\*10\*2048 feature map on its last feature extractor layer from the input image, and ResNet50V2 also produces the same size of feature map on its final layer. As both networks generate the same size of feature maps, we concatenated their features so that by using both of the inception-based layers and residual-based layers, the quality of the generated semantic features be enhanced.

The concatenated neural network is designed by concatenating the extracted features of Xception and ResNet50V2 and then connecting the concatenated features to a convolutional layer that is connected to the classifier. The kernel size of the convolutional layer that was added after the concatenated features was 1\*1 with 1024 filters and no activation function. This layer was added to extract a more valuable semantic feature out of the features of a spatial point between all the channels, which each channel is a feature map. This convolutional layer helps the network learn better from the concatenated features extracted from Xception and ResNet50V2. The architecture of the concatenated network has been depicted in figure 1.

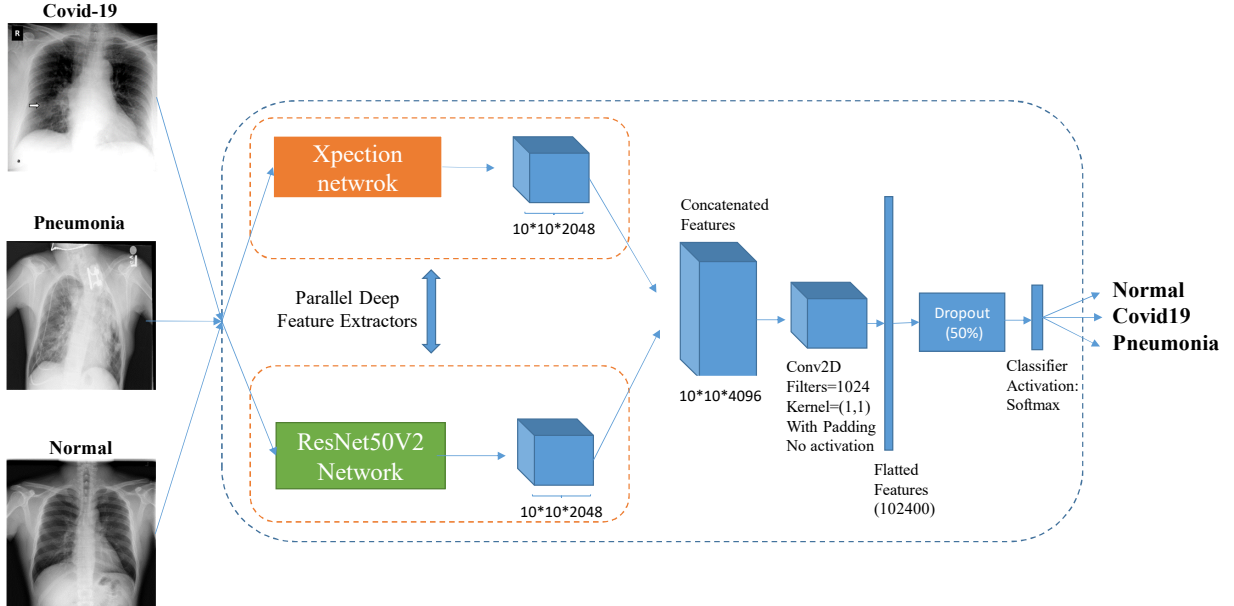


Figure 1: The architecture of the concatenated network

## 2.2 Dataset

We have used two open-source datasets in our work. The covid chestxray dataset is taken from this GitHub repository (<https://github.com/ieee8023/covid-chestxray-dataset>), which has been prepared by [6]. This dataset consists of X-ray and CT scan images of patients infected to COVID-19, SARS, Streptococcus, ARDS, Pneumocystis, and other types of pneumonia from different patients.

In this dataset, we only considered the x-ray images, and in total, there were 180 images from 118 cases with COVID-19 and 42 images from 25 cases with Pneumocystis, Streptococcus, and SARS that were considered as pneumonia. The second dataset was taken from (<https://www.kaggle.com/c/rsna-pneumonia-detection-challenge>), which contains 6012 cases with pneumonia, and 8851 normal cases. We combined these two datasets, and the details are listed in table 1.

Table 1: Composition of the number of allocated images to training and validation set in both datasets

Dataset	COVID-19	Pneumonia	Normal
covid chestxray dataset	180	42	0
rsna pneumonia detection challenge	0	6012	8851
Total	180	6054	8851
Training Set	149	1634	2000
Validation Set	31	4420	6851

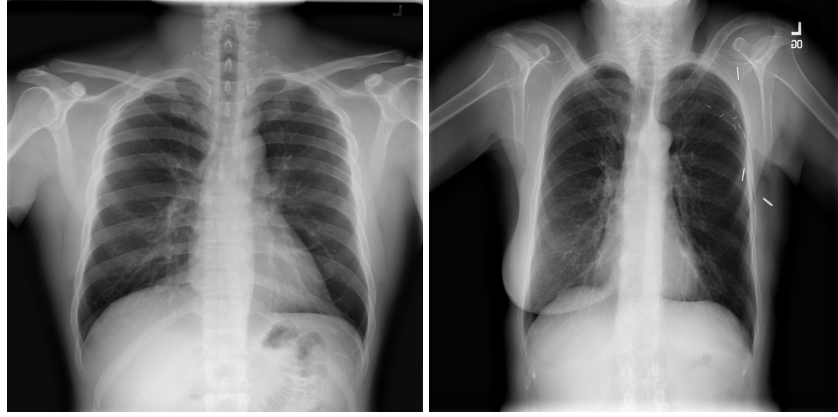
As stated, we only had 180 cases infected to COVID-19, which is almost a few data for a class compared to other classes. If we had combined lots of images from normal or pneumonia classes with few COVID-19 images for training, the network would become able to detect pneumonia and normal classes very well, but not the COVID-19 class because of the unbalanced dataset. In that case, although the network can not identify COVID-19 properly, as there are many more images of pneumonia and normal classes than the COVID-19 class, the general accuracy would become very high, not the COVID-19 detection accuracy. This condition is not our goal because the main purpose here is to achieve good results in detecting COVID-19 cases and not identifying wrong COVID-19 cases.

The best way to solve this problem is to make the dataset balanced and give the network almost equal data of each class when training, so the network learn to identify all the classes. Here because we do not access more open-source datasets of COVID-19 to increase this class data, we chose the number of pneumonia and normal classes almost equal to the COVID-19 number of images.

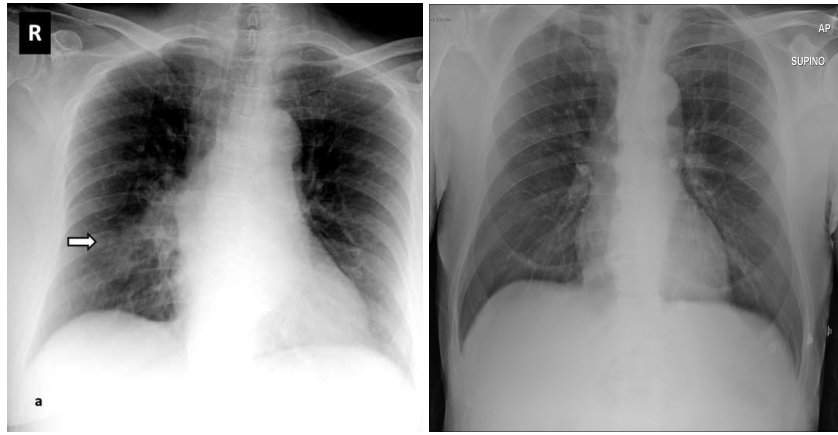
We decided to train the networks for 8 consecutive phases. In each phase, we selected 250 cases of normal class and 234 cases of pneumonia class along with the 149 COVID-19 cases. In total, we had 633 cases for each training phase. All the COVID-19 images and 34 of the pneumonia images were common between each training phase and 250 normal cases, and 200 pneumonia cases were unique in each training phase. The common 149 COVID-19 and 34 pneumonia cases between all the training phases were from the covid chestxray dataset [6], and the rest of the data were from the other dataset. Based on this categorizing, our training set includes 8 phases and 3783 images.

By doing so, the network sees an almost equal number of images for each class, so it helps to improve the COVID-19 detection along detecting pneumonia and normal cases. But as we had more pneumonia and normal cases, we showed the network different pneumonia and normal cases with COVID-19 cases in each phase. Implementing this method results in two advantages. One is that the network learns COVID-19 class features better along with the other classes; second, the normal and pneumonia classes' detection improves very much. Better detecting pneumonia and normal cases mean not detecting wrong COVID-19 cases, which is one of our goals. In another meaning running this method helps the network better identify COVID-19 and not detect faulty COVID-19 cases.

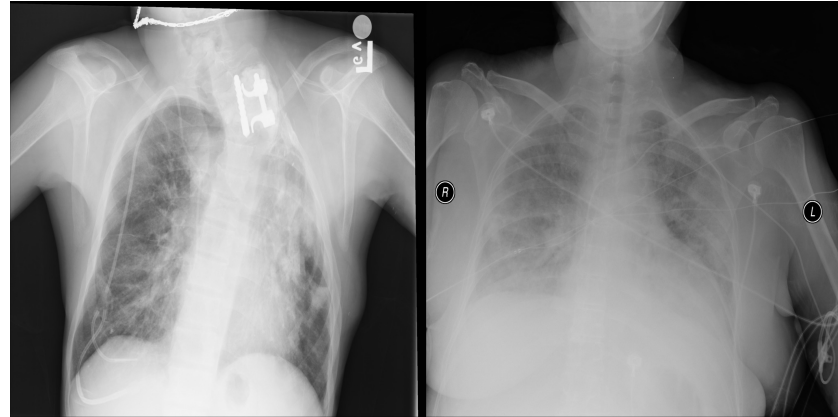
This method can be used for all the circumstances that there is a highly unbalanced dataset. We presented our way of allocating the images of the datasets into eight different phases in flowchart 3. Some of the images of our dataset are shown in figure 2.



(a) normal persons



(b) Patients with COVID-19



(c) Patients with pneumonia

Figure 2: Examples of the images in our dataset

### 2.3 Training phase

We described in the dataset subsection 2.2 that we allocated 8 phases for training. For reporting more reliable results, we chose five folds for training, which in every fold the training set was made of 8 phases as it is mentioned.

We have trained ResNet50V2 [11], Xception [4], and a concatenation of Xception and ResNet50V2 neural networks based on the explained method. This concatenated Neural Network has shown higher accuracy comparing to the others.

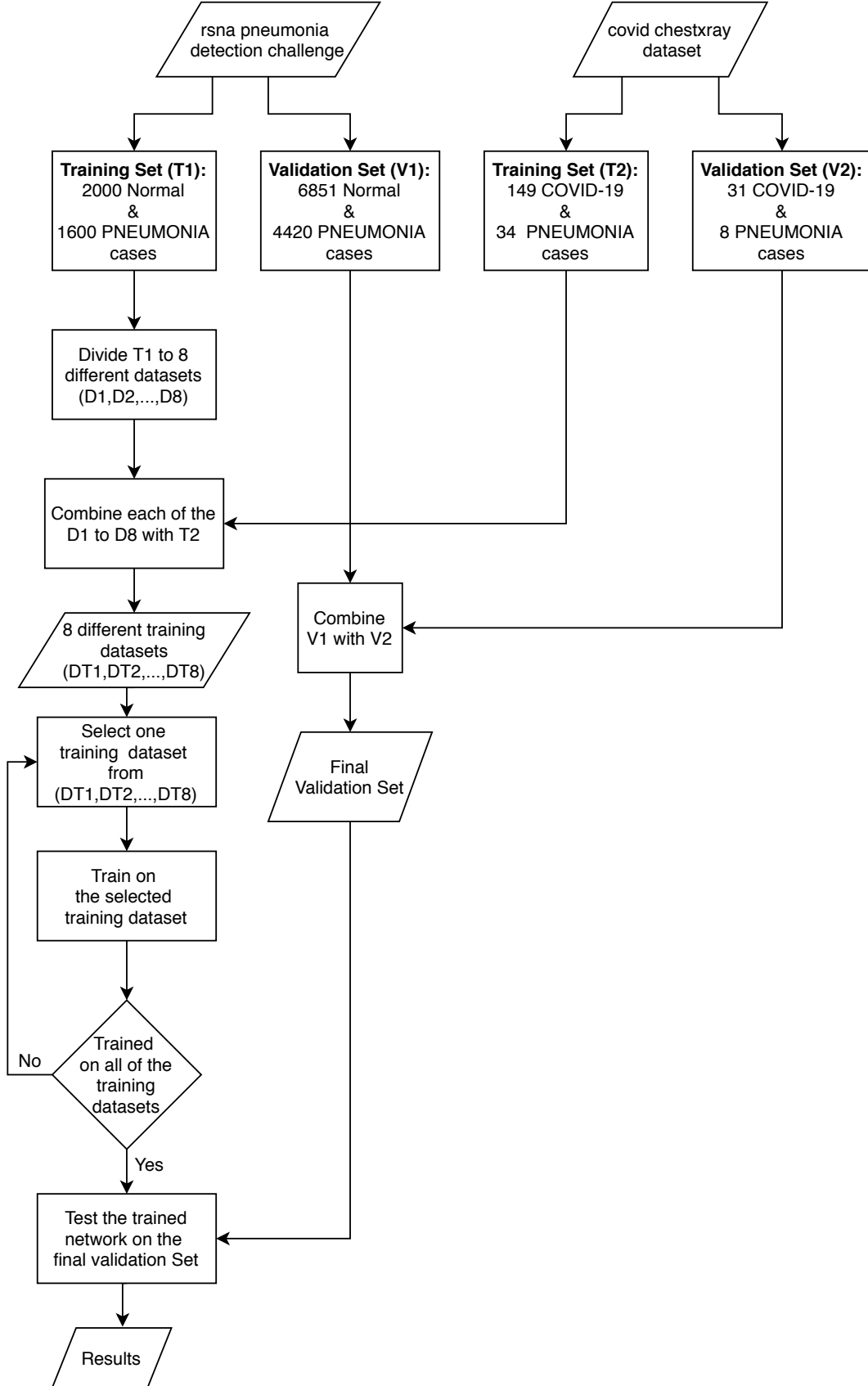


Figure 3: The flowchart of the proposed method for training set preparation

As we have tested several networks in our project, the Xception [4] and ResNet50V2 [11] networks work almost better than other ones in extracting deep features. By concatenating the output features of both networks, we helped the network learn to classify the input image from both feature vectors, which resulted in better accuracy. The training parameters have been described in table 2.

Based on table 2 we trained the networks using Categorical cross-entropy loss function and Nadam optimizer. The learning rate was set to  $1e-4$ . We trained the network for 100 epochs in each training phase and, because of having 8 training phases, the models were trained for 800 epochs. For the Xception and ResNet50V2, we selected the batch size equal to 30. But as the concatenated network had more parameters than Xception and ResNet50V2, we set the batch size equal to 20. Data augmentation methods were also implemented to increase training efficiency and prevent the model from overfitting.

We implemented the neural networks with Keras [5] library on a Tesla P100 GPU and 25GB RAM that were provided by [Google Colaboratory Notebooks](#).

Table 2: In this table, we have listed the parameters and functions we used in the training procedure.

Training Parameters	Xception	ResNet50V2	Concatenated Network
Learning Rate	$1e-4$	$1e-4$	$1e-4$
Batch Size	30	30	20
Optimizer	Nadam	Nadam	Nadam
Loss Function	Categorical Crossentropy	Categorical Crossentropy	Categorical Crossentropy
Epochs per each Training Phase	100	100	100
Horizontal/Vertical flipping	Yes	Yes	Yes
Zoom Range	5%	5%	5%
Rotation Range	0 - 360 degree	0 - 360 degree	0 - 360 degree
Width / Height Shifting	5%	5%	5%
Shift Range	5%	5%	5%
Re-scaling	1/255	1/255	1/255

### 3 Results

We validated our networks on 31 cases of COVID-19, 4420 cases of pneumonia, and 6851 normal cases. The reason our training data was less than validation data is that we had a few cases of COVID-19 among lots of normal and with pneumonia cases. Therefore, we could not use lots of images of the two other classes with COVID-19 fewer cases for training because it would have made the network not to learn COVID-19 features. To solve this issue, we selected 3783 images for training in 8 different phases. We evaluated our network on the rest of the data so that our trained network's ultimate performance be clear. It must be noticed that exceptionally, in the fold3, we had 30 cases of COVID-19 for validation, and 150 other cases were allocated for training.

It is noteworthy that we used transfer learning in training process. For all the networks, we used the pre-trained ImageNet weights [8] at the beginning of the training and then resumed training based on the explained conditions on our dataset. We also used the accuracy metric for monitoring the network results on the validation set after each epoch to find the best and most converged version of the trained network.



The evaluation results of the neural networks are presented in figure 4 that shows the confusion matrices of each network for fold one and three. Table 3 and table 4 show the details of our results. We reported the four different metrics for evaluating our network for each of the three class as follows:

$$Accuracy (for each class) = \frac{TP + TN}{TP + FP + TN + FN} \quad (1)$$

$$Specificity = \frac{TN}{TN + FP} \quad (2)$$

$$sensitivity = \frac{TP}{TP + FN} \quad (3)$$

$$Precision = \frac{TP}{TP + FP} \quad (4)$$

We also reported the overall accuracy metric, defined as:

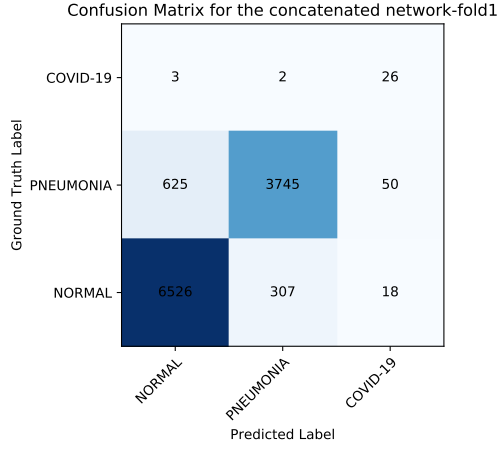
$$Accuracy (for all the classes) = \frac{Number\ of\ Correct\ Classified\ Images}{Number\ of\ All\ Images} \quad (5)$$

In these equations,  $TP$  (True Positive) is the number of correctly classified images of a class,  $FP$  (False Positive) is the number of the wrong classified images of a class,  $FN$  (False Negative) is the number of images of a class that have been detected as another class, and  $TN$  (True Negative) is the number of images that do not belong to a class and did not be classified as that class.

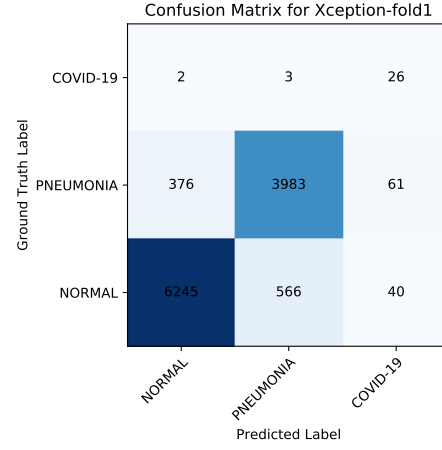
Table 3: This table reports the number of true and false positives and false negatives for each class

Fold	Network	COVID-19 Correct detected	COVID-19 Not detected	COVID-19 Wrong detected	PNEUMONIA Correct detected	PNEUMONIA Not detected	PNEUMONIA Wrong detected	NORMAL Correct detected	NORMAL Not detected	NORMAL Wrong detected
1	Xception	26	5	101	3983	437	569	6245	606	378
	ResNet50V2	27	4	96	3858	562	480	6334	517	507
	Concatenated	26	5	68	3745	675	309	6526	325	628
2	Xception	23	8	42	3874	546	409	6426	425	528
	ResNet50V2	22	9	67	3659	761	501	6340	511	713
	Concatenated	23	8	27	3913	507	434	6413	438	492
3	Xception	21	9	28	3942	478	436	6411	440	463
	ResNet50V2	22	8	97	3770	650	392	6433	418	587
	Concatenated	25	5	35	3847	573	342	6502	349	550
4	Xception	22	9	42	3818	602	433	6411	440	576
	ResNet50V2	22	9	78	4015	405	758	6065	786	364
	Concatenated	26	5	77	3860	560	480	6340	511	519
5	Xception	21	10	41	4041	379	502	6335	516	362
	ResNet50V2	21	10	42	3604	816	284	6549	302	802
	Concatenated	24	7	43	3941	479	390	6442	409	462

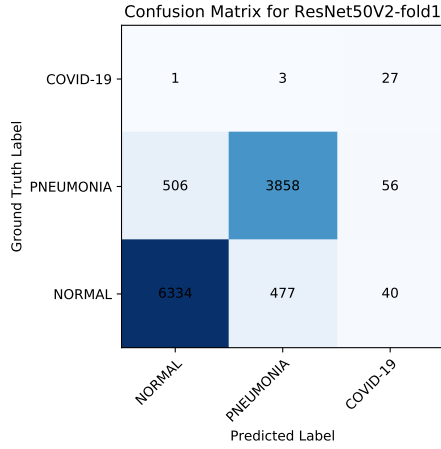




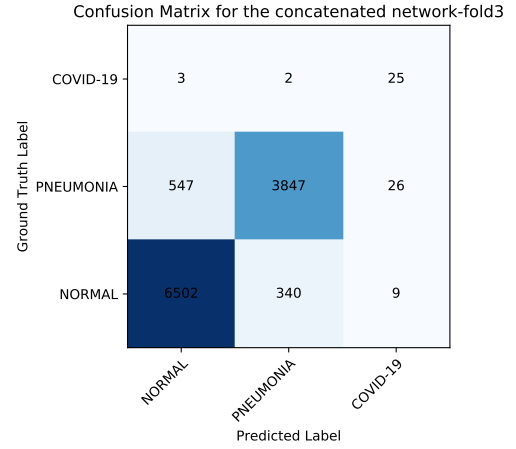
(a) Concatenated network-Fold1



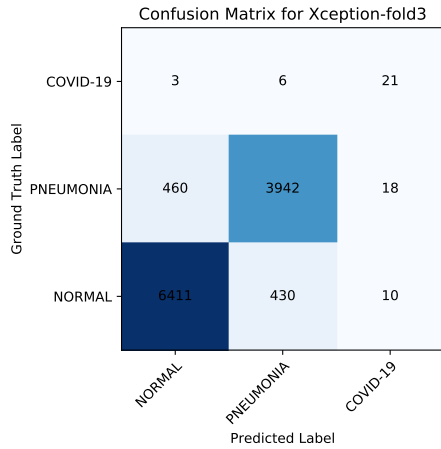
(b) Xception-Fold1



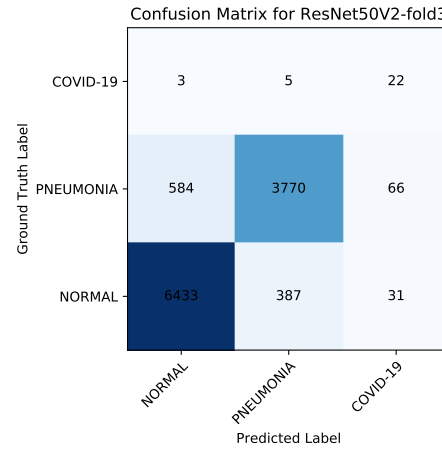
(c) ResNet50V2-Fold1



(d) Concatenated network-Fold3



(e) Xception-Fold3



(f) ResNet50V2-Fold3

Figure 4: This figure shows the confusion matrix of the network for fold 1 and 3

Table 4: Some of the evaluation metrics have been reported in this table.

Fold	Network	Accuracy	COVID-19 sensitivity	PNEUMONIA sensitivity	NORMAL sensitivity	COVID-19 Specificity	PNEUMONIA Specificity	NORMAL Specificity	COVID-19 Accuracy	PNEUMONIA Accuracy	NORMAL Accuracy	COVID-19 Precision	PNEUMONIA Precision	NORMAL Precision
1	Xception	90.72	83.87	90.11	91.15	99.1	91.73	91.51	99.06	91.10	91.29	20.47	87.50	94.29
	ResNet50V2	90.41	87.09	87.28	92.45	99.15	93.03	88.61	99.12	90.78	90.94	21.95	88.93	92.58
	Concatenated	91.10	83.87	84.72	95.25	99.4	95.51	85.89	99.35	91.29	91.57	27.65	92.37	91.22
2	Xception	91.33	74.19	87.64	93.79	99.63	94.06	88.14	99.56	91.55	91.57	35.38	90.45	92.40
	ResNet50V2	88.66	70.96	82.78	92.54	99.41	92.72	83.98	99.33	88.83	89.17	24.71	87.95	89.89
	Concatenated	91.56	74.19	88.52	93.60	99.76	93.69	88.95	99.69	91.67	91.77	46	90.01	92.87
3	Xception	91.79	70	89.18	93.57	99.75	93.66	89.6	99.67	91.91	92.01	42.85	90.04	93.26
	ResNet50V2	90.47	73.33	85.29	93.89	99.14	94.30	86.81	99.07	90.78	91.11	18.48	90.58	91.63
	Concatenated	91.79	83.33	87.03	94.90	99.69	95.03	87.64	99.65	91.90	92.04	41.66	91.83	92.20
4	Xception	90.70	70.96	86.38	93.57	99.63	93.71	87.06	99.55	90.84	91.01	34.37	89.81	91.75
	ResNet50V2	89.38	70.96	90.83	88.52	99.31	88.99	91.82	99.23	89.71	89.82	22	84.11	94.33
	Concatenated	90.47	83.87	87.33	92.54	99.32	93.03	88.34	99.27	90.8	90.89	25.24	88.94	92.43
5	Xception	91.99	67.74	91.42	92.46	99.64	92.71	91.87	99.55	92.20	92.23	33.87	88.95	94.59
	ResNet50V2	90.01	67.74	81.53	95.59	99.63	95.87	81.98	99.54	90.27	90.23	33.33	92.69	89.08
	Concatenated	92.08	77.41	89.16	94.03	99.62	94.33	89.62	99.56	92.31	92.29	35.82	90.99	93.30
Average	Xception	91.31	73.35	88.95	92.91	99.55	93.17	89.63	99.48	91.52	91.62	33.39	89.35	93.26
	ResNet50V2	89.79	74.02	85.54	92.60	99.33	92.98	86.64	99.26	90.07	90.25	24.09	88.85	91.50
	Concatenated	91.40	80.53	87.35	94.06	99.56	94.32	88.09	99.50	91.60	91.71	35.27	90.83	92.40

## 4 Discussion

It can be understood from the confusion matrices and the tables that the concatenated network performs better in detecting COVID-19 and not detecting false cases of COVID-19 and outputs better overall accuracy. Although we had an unbalanced dataset and a few cases of COVID-19, by using the proposed technique, we could have improved COVID-19 detection along with the other classes detection. The reason the precision of COVID-19 class is low is that in our work, despite some other researches that worked on detecting COVID-19 from X-ray images, we tested our neural nets on a massive number of images. Our test images were much more than our train images. As it is explained above, because we had only 31 cases of COVID-19 and 11271 cases from the other two classes, the false positives of the COVID-19 class would become more than true positives. For example, in the first fold, the concatenated network detected 26 cases correctly out of 31 COVID-19 cases, and from 11271 other cases, only mistakenly identify 68 cases as COVID-19. If we had equal samples from COVID-19 class as the other classes, the precision would become high value. Still, because having few COVID-19 cases and lots of other cases for validation, the precision would become a low value.

In another study, the results were presented in two forms, 2 and 3 classes, that due to the imbalance in the dataset, there are several meaningless results [2]. We have presented the results for each class and for all the classes with meaningful results that are more practical. We could have tested our network on a few cases like some of the other researches done recently, but we wanted to show the real performance of our network with few COVID-19 cases. As mentioned, mistakenly detecting 68 cases from 11271 cases to be infected to COVID-19 is not very much but not very well also, and we hope that by using much-provided data from patients infected, COVID-19, the detection accuracy will rise much more.

## 5 Conclusion

In this paper, we presented a concatenated neural network based on Xception and ResNet50V2 networks for classifying the chest X-ray images into three categories of normal, pneumonia, and COVID-19. We used two open-source datasets that contained 180 and 6054 images from patients infected to COVID-19 and pneumonia, respectively, and 8851 images from normal people. As we had a few images of COVID-19 class, we proposed a method for training the neural network when the dataset is unbalanced. We separated the training set into 8 successive phases, in which there were 633 images (149 COVID-19, 234 pneumonia, 250 normal) in each phase. We selected the number of each class almost equal to each other in each phase so that our network also learns COVID-19 class characteristics, not only the other two class features. In each phase, the images from normal and pneumonia classes were different so that the network can distinguish COVID-19 from other classes better. Our training set included 3783 images, and the rest of the images were

allocated for evaluating the network. We tried to test our model on a large number of images so that our real achieved accuracy be clear. We achieved an average accuracy of 99.50%, and 80.53% sensitivity for the COVID-19 class, and the overall accuracy equal to 91.4% between five folds. We hope that our trained network that is publicly available be helpful for medical diagnosis. We also hope that in the future, larger datasets from COVID-19 patients become available, and by using them, the accuracy of our proposed network increases for good.

## 6 Code Availability

In this GitHub profile (<https://github.com/mr7495/covid19>), we have shared the trained networks and all the used code in this paper. We hope our work be useful to help in future researches.

## Acknowledgment

We would like to appreciate Joseph Paul Cohen and the others who provided these x-ray images from patients infected to COVID-19. We thank Linda Wang and Alexander Wong for making their code available, in which we have used a part of it on our research for preparing our dataset. We also thank [Google Colab server](#) for providing free GPU.

This is a preprint of an article published in Informatics in Medicine Unlocked journal. The final authenticated version is available online at [10.1016/j.imu.2020.100360](https://doi.org/10.1016/j.imu.2020.100360).

## References

- [1] P. An, H. Chen, X. Jiang, J. Su, Y. Xiao, Y. Ding, H. Ren, M. Ji, Y. Chen, W. Chen, et al. Clinical features of 2019 novel coronavirus pneumonia presented gastrointestinal symptoms but without fever onset. *arxiv*, 2020.
- [2] I. D. Apostolopoulos and T. A. Mpesiana. Covid-19: automatic detection from x-ray images utilizing transfer learning with convolutional neural networks. *Physical and Engineering Sciences in Medicine*, page 1, 2020.
- [3] J.-Z. Cheng, D. Ni, Y.-H. Chou, J. Qin, C.-M. Tiu, Y.-C. Chang, C.-S. Huang, D. Shen, and C.-M. Chen. Computer-aided diagnosis with deep learning architecture: applications to breast lesions in us images and pulmonary nodules in ct scans. *Scientific reports*, 6(1):1–13, 2016.
- [4] F. Chollet. Xception: Deep learning with depthwise separable convolutions. In *Proceedings of the IEEE conference on computer vision and pattern recognition*, pages 1251–1258, 2017.
- [5] F. Chollet and Others. keras, 2015.
- [6] J. P. Cohen, P. Morrison, and L. Dao. Covid-19 image data collection. *arXiv preprint arXiv:2003.11597*, 2020.
- [7] J. Dekhtiar, A. Durupt, M. Bricogne, B. Eynard, H. Rowson, and D. Kiritsis. Deep learning for big data applications in cad and plm—research review, opportunities and case study. *Computers in Industry*, 100:227–243, 2018.
- [8] J. Deng, W. Dong, R. Socher, L.-J. Li, K. Li, and L. Fei-Fei. Imagenet: A large-scale hierarchical image database. In *2009 IEEE conference on computer vision and pattern recognition*, pages 248–255. Ieee, 2009.
- [9] O. Gozes, M. Frid-Adar, H. Greenspan, P. D. Browning, H. Zhang, W. Ji, A. Bernheim, and E. Siegel. Rapid ai development cycle for the coronavirus (covid-19) pandemic: Initial results for automated detection & patient monitoring using deep learning ct image analysis. *arXiv preprint arXiv:2003.05037*, 2020.
- [10] K. He, X. Zhang, S. Ren, and J. Sun. Deep residual learning for image recognition, 2015.
- [11] K. He, X. Zhang, S. Ren, and J. Sun. Identity mappings in deep residual networks. In *European conference on computer vision*, pages 630–645. Springer, 2016.
- [12] G. Huang, Z. Liu, L. van der Maaten, and K. Q. Weinberger. Densely connected convolutional networks, 2016.
- [13] F. Jiang, L. Deng, L. Zhang, Y. Cai, C. W. Cheung, and Z. Xia. Review of the clinical characteristics of coronavirus disease 2019 (covid-19). *Journal of General Internal Medicine*, pages 1–5, 2020.
- [14] S. Lakshmanprabu, S. N. Mohanty, K. Shankar, N. Arunkumar, and G. Ramirez. Optimal deep learning model for classification of lung cancer on ct images. *Future Generation Computer Systems*, 92:374–382, 2019.
- [15] L. Li, L. Qin, Z. Xu, Y. Yin, X. Wang, B. Kong, J. Bai, Y. Lu, Z. Fang, Q. Song, et al. Artificial intelligence distinguishes covid-19 from community acquired pneumonia on chest ct. *Radiology*, page 200905, 2020.
- [16] O. S. Lih, V. Jahmunah, T. R. San, E. J. Ciaccio, T. Yamakawa, M. Tanabe, M. Kobayashi, O. Faust, and U. R. Acharya. Comprehensive electrocardiographic diagnosis based on deep learning. *Artificial Intelligence in Medicine*, 103:101789, 2020.

- [17] G. Litjens, T. Kooi, B. E. Bejnordi, A. A. A. Setio, F. Ciompi, M. Ghafoorian, J. A. Van Der Laak, B. Van Ginneken, and C. I. Sánchez. A survey on deep learning in medical image analysis. *Medical image analysis*, 42:60–88, 2017.
- [18] K. McIntosh. *Coronavirus disease 2019 (COVID-19): Epidemiology, virology, clinical features, diagnosis, and prevention*, 2020-04-10.
- [19] W. Meters. *COVID-19 CORONAVIRUS PANDEMIC* <https://www.worldometers.info/coronavirus>, 2020-04-10.
- [20] A. Narin, C. Kaya, and Z. Pamuk. Automatic detection of coronavirus disease (covid-19) using x-ray images and deep convolutional neural networks. *arXiv preprint arXiv:2003.10849*, 2020.
- [21] B. Pirouz, S. Shaffiee Haghshenas, B. Pirouz, S. Shaffiee Haghshenas, and P. Piro. Development of an assessment method for investigating the impact of climate and urban parameters in confirmed cases of covid-19: A new challenge in sustainable development. *International Journal of Environmental Research and Public Health*, 17(8):2801, 2020.
- [22] B. Pirouz, S. Shaffiee Haghshenas, S. Shaffiee Haghshenas, and P. Piro. Investigating a serious challenge in the sustainable development process: analysis of confirmed cases of covid-19 (new type of coronavirus) through a binary classification using artificial intelligence and regression analysis. *Sustainability*, 12(6):2427, 2020.
- [23] M. Rahimzadeh and A. Attar. Introduction of a new dataset and method for detecting and counting the pistachios based on deep learning. *arXiv preprint arXiv:2005.03990*, 2020.
- [24] M. Rahimzadeh, A. Attar, et al. Sperm detection and tracking in phase-contrast microscopy image sequences using deep learning and modified csr-dcf. *arXiv preprint arXiv:2002.04034*, 2020.
- [25] O. Ronneberger, P. Fischer, and T. Brox. U-net: Convolutional networks for biomedical image segmentation. In *International Conference on Medical image computing and computer-assisted intervention*, pages 234–241. Springer, 2015.
- [26] F. Shan+, Y. Gao+, J. Wang, W. Shi, N. Shi, M. Han, Z. Xue, D. Shen, and Y. Shi. Lung infection quantification of covid-19 in ct images with deep learning. *arXiv preprint arXiv:2003.04655*, 2020.
- [27] K. Simonyan and A. Zisserman. Very deep convolutional networks for large-scale image recognition, 2014.
- [28] F. Song, N. Shi, F. Shan, Z. Zhang, J. Shen, H. Lu, Y. Ling, Y. Jiang, and Y. Shi. Emerging 2019 novel coronavirus (2019-ncov) pneumonia. *Radiology*, page 200274, 2020.
- [29] D. Sun, H. Li, X.-X. Lu, H. Xiao, J. Ren, F.-R. Zhang, and Z.-S. Liu. Clinical features of severe pediatric patients with coronavirus disease 2019 in wuhan: a single center’s observational study. *World Journal of Pediatrics*, pages 1–9, 2020.
- [30] C. Szegedy, S. Ioffe, V. Vanhoucke, and A. Alemi. Inception-v4, inception-resnet and the impact of residual connections on learning, 2016.
- [31] C. Szegedy, W. Liu, Y. Jia, P. Sermanet, S. Reed, D. Anguelov, D. Erhan, V. Vanhoucke, and A. Rabinovich. Going deeper with convolutions, 2014.
- [32] univers1. *Everything about the Corona virus* <https://medicine-and-mental-health.xyz/archives/4510>, 2020-04-12.
- [33] L. Wang and A. Wong. Covid-net: A tailored deep convolutional neural network design for detection of covid-19 cases from chest radiography images. *arXiv preprint arXiv:2003.09871*, 2020.
- [34] S. Wang, B. Kang, J. Ma, X. Zeng, M. Xiao, J. Guo, M. Cai, J. Yang, Y. Li, X. Meng, et al. A deep learning algorithm using ct images to screen for corona virus disease (covid-19). *medRxiv*, 2020.
- [35] X. Wang, H. Qian, E. J. Ciaccio, S. K. Lewis, G. Bhagat, P. H. Green, S. Xu, L. Huang, R. Gao, and Y. Liu. Celiac disease diagnosis from videocapsule endoscopy images with residual learning and deep feature extraction. *Computer Methods and Programs in Biomedicine*, 187:105236, 2020.
- [36] WHO. <https://www.who.int>, 2020-04-10.
- [37] X. Xu, X. Jiang, C. Ma, P. Du, X. Li, S. Lv, L. Yu, Y. Chen, J. Su, G. Lang, et al. Deep learning system to screen coronavirus disease 2019 pneumonia. *arXiv preprint arXiv:2002.09334*, 2020.
- [38] R. Yang, X. Li, H. Liu, Y. Zhen, X. Zhang, Q. Xiong, Y. Luo, C. Gao, and W. Zeng. Chest ct severity score: An imaging tool for assessing severe covid-19. *Radiology: Cardiothoracic Imaging*, 2(2):e200047, 2020.
- [39] B. Zoph, V. Vasudevan, J. Shlens, and Q. V. Le. Learning transferable architectures for scalable image recognition, 2017.

- [40] M. Zreik, N. Lessmann, R. W. van Hamersvelt, J. M. Wolterink, M. Voskuil, M. A. Viergever, T. Leiner, and I. Išgum. Deep learning analysis of the myocardium in coronary ct angiography for identification of patients with functionally significant coronary artery stenosis. *Medical image analysis*, 44:72–85, 2018.